Dielectric Concentrator for Cherenkov Radiation

Sergey N. Galyamin* and Andrey V. Tyukhtin†
Physical Faculty, St. Petersburg State University, St. Petersburg 198504, Russia
(Received 20 March 2014; published 7 August 2014)

We report on a dielectric target that concentrates Cherenkov radiation into a small spatial area. In contrast to traditional devices, this target can focus almost all of the radiation without using additional lenses or mirrors. We consider the case where radiation is produced by a point charge moving along the axis of a cylindrical channel inside an axially symmetrical target. The specific form of the target is determined using the laws of ray optics. The field is calculated using an aperture integration method that can determine the field near the focus. Typical field plots and the spatial distribution of the field outside the target are presented. We demonstrate that at terahertz frequencies, this concentrator can increase the field magnitude by up to at least 2 orders of magnitude relative to that on the surface of the target.

DOI: 10.1103/PhysRevLett.113.064802 PACS numbers: 41.60.Bq, 42.15.-i, 42.25.Gy

Cherenkov radiation (CR) is a well-known and widely applied phenomenon. One important application of this effect is the detection of charged particles [1,2]. Interesting applications of CR can be found in various fields; these applications include bunch diagnostics [3,4], wakefield acceleration [5,6], terahertz radiation sources [7–9], and Cherenkov luminescence tomography [10] etc. Frequently, it is important to concentrate the CR energy into specific small spatial areas. Various additional lenses or mirrors that refract or reflect, respectively, the CR are typically used to concentrate the CR. However, a target with a specific geometry can be created that combines the radiator and the concentrator into a single device. This type of effect is discussed in this paper.

Note that the rigorous theory of CR is only well developed for a number of rather simple cases, such as infinite (borderless) media and regular waveguide structures [1,2,11,12]. However, in realistic cases, the geometry of the actual radiating structure frequently does not allow for an exact analytical solution of the electromagnetic field. To calculate the radiated field in these complicated cases, various approximation techniques are utilized [3,9,13–15]. In this paper, the shape of the concentrating target is determined using the combined method suggested in our recent paper [15], which utilizes the exact solution of certain "key" problem and the laws of ray optics. Furthermore, we also use another approach (an aperture integration technique known from antenna theory [16]) to calculate the field near the focus, where ray optics fails.

We address the problem shown in Fig. 1(a). Let a point charge q travel with a constant velocity $v = \beta c$ in a vacuum in a cylindrical channel (of radius a) in an axially symmetrical dielectric target (with real permittivity ε, real permeability μ, and the corresponding refractive index $n = \sqrt{\varepsilon\mu} > 1$). A target shape $r(\theta)$ should be found that concentrates the radiation produced by the charge at a given frequency ω onto a focus point situated on the axis: $x = y = 0$, $z = z_f$.

First, to determine the field inside the target, we utilize the approximation method suggested in our recent paper [15]. This field is accepted to be the same as that in the corresponding "key" problem: a point charge travels along the vacuum channel in an unbounded medium with permittivity ε and permeability μ [Fig. 1(b)]. An exact solution of the Fourier transform of the magnetic field is [12]

$$H_{\varphi\omega} = -q(\pi a c)^{-1}\eta^{-1} s H_1^{(1)}(\rho s)\exp(i\omega z/v),$$
$$\eta = \frac{\varepsilon\mu\beta^2 - 1}{\varepsilon(1-\beta^2)} s_0 I_1(s_0 a) H_0^{(1)}(sa) - s I_0(s_0 a) H_1^{(1)}(sa), \quad (1)$$

where $s = \omega v^{-1}\sqrt{\varepsilon\mu\beta^2 - 1}$, $s_0 = |\omega| v^{-1}\sqrt{1-\beta^2}$, $\rho = \sqrt{x^2 + y^2}$, $H_{0,1}^{(1)}$ and $I_{0,1}$ are the Hankel function and the modified Bessel functions, respectively. Second, we should describe the interaction between the Cherenkov radiation (1) and the target surface. This interaction can be described using ray optics techniques. For large ρ ($\rho|s| \gg 1$), the phase of the Cherenkov wave (in units of $k = \omega/c$) is

$$\psi = \beta^{-1}\left(z + \sqrt{\varepsilon\mu\beta^2 - 1}\rho\right). \quad (2)$$

Therefore, the angle of the Cherenkov radiation front α is determined by $\sin\alpha = (n\beta)^{-1}$. The wave front and the corresponding rays inside the target can be easily obtained [see Fig. 1(b)]. The terms of the problem indicate that all the rays should converge to the focus after they are transmitted from the boundary.

To determine the shape of the surface that performs this task, we consider this problem from another viewpoint. First, we expand the ray picture from the "upper" part of the

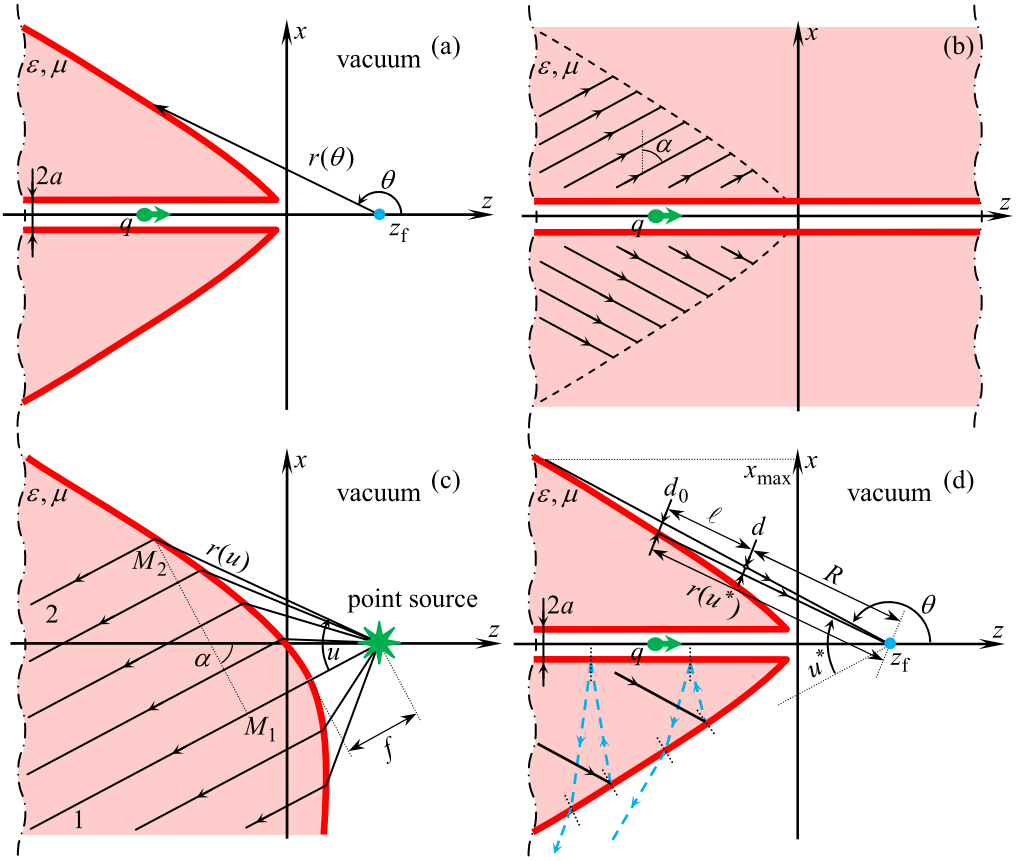

FIG. 1 (color online). (a) Geometry of the problem: the target shape $r(\theta)$ is such that the target concentrates the CR onto the focus. (b) Geometry and rays of the "key" problem: CR from a charge moving in a cylindrical channel in an unbounded medium. (c) Geometry and rays of the "expanded" problem: a point source is placed at the focus, and the surface that transforms the divergent ray beam into a parallel beam is determined. (d) Final target that is extracted from the expanded target (c), two narrow rays (black solid) that converge to the focus point, and two multiple reflected rays (blue dashed) that do not converge to the focus.

target to the whole plane, as shown in Fig. 1(c). Second, we flip the rays by supposing that a point source is located at the point $x = y = 0$, $z = z_f$. Next, we are left with the problem of finding the surface that transforms the divergent bunch of rays to a parallel bunch. Fortunately, the solution to this problem is known from antenna theory [16]. From a physical point of view, the fact that the rays become parallel after refraction means that the optical path difference for two arbitrary rays is equal to zero. Using ray 1 (which is orthogonal to the front and does not refract) and another ray 2 [see Fig. 1(c)], we obtain the following for the difference in the optical length for points M_1 and M_2:

$$r - [f + (r\cos u - f)n] = 0, \tag{3}$$

where f is the shortest distance from the source to the surface (along ray 1), and the angle u is measured from ray 1. From (3), we find

$$r(u) = f(1-n)/[1 - n\cos u]. \tag{4}$$

Formula (4) describes a hyperbola with asymptotes $u = \pm u_a = \cos^{-1}(1/n)$. For simplicity, we choose f so that the curve (4) crosses the z axis at $z = 0$. Note that other curves also exist that provide a parallel ray bunch after refraction. These curves are obtained from (4) by substituting $f(1-n)$ with $f(1-n) + m\lambda$, where m is an integer, and λ is the wavelength in vacuum (see [16] for detail).

We return to the initial problem and extract the section for $u \in [u_{min}, u_{max}]$ from the whole curve $r(u)$. Here, $u_{min} > \pi/2 - \alpha$ is determined by the radius a of the channel, and $u_{max} < u_a$ is determined using the target dimensions. Finally, we rotate this piece about the z axis and obtain the following system that specifies the refracting surface:

$$\rho_0(u) = -r(u)\cos(u + \alpha),$$
$$z_0(u) = z_f - r(u)\sin(u + \alpha). \tag{5}$$

The values u_{min} and u_{max} should be determined from $\rho_0(u_{min}) = a$ and $\rho_0(u_{max}) = \rho_{max}$, where ρ_{max} is the maximum orthogonal dimension of the target [Fig. 1(d)].

We can calculate the ray geometry using (4) and (5) along with the V. A. Fock method [17], which describes the interaction between an arbitrary wave and an arbitrary surface. For each observation point determined by the coordinates R and θ, we should find the point u^* at the target surface from which the corresponding ray originates. One obtains

$$u^* = 3\pi/2 - \alpha - \theta \quad \text{for } \theta \in [\pi/2, \pi],$$
$$u^* = \pi/2 - \alpha + \theta \quad \text{for } \theta \in [0, \pi/2]. \tag{6}$$

where $\theta \in [\pi/2, \pi]$ corresponds to the area in front of the focus, and $\theta \in [0, \pi/2]$ corresponds to the area behind the focus. Note that the value of u^* calculated from (6) should be between $u_{\min}$ and $u_{\max}$; otherwise, the ray is absent for the given observation point. In vacuum, the ray length l is

$$l = r(u^*) - R \quad \text{for } \theta \in [\pi/2, \pi],$$
$$l = r(u^*) + R \quad \text{for } \theta \in [0, \pi/2]. \tag{7}$$

Nonzero components of the field are calculated using the following formulas:

$$H_{\varphi\omega} = -E_{\theta\omega} = H^*_{\varphi\omega} T_{\parallel} \sqrt{D(0)/D(l)}\, \exp(i\omega l/c), \tag{8}$$

where $H^*_{\varphi\omega}$ is the field (1) at the point where the ray originates, and $T_{\parallel}$ is the transmission coefficient:

$$T_{\parallel} = 2n \cos\theta_{\mathrm{i}} [n \cos\theta_{\mathrm{i}} + \cos\theta_{\mathrm{t}}]^{-1}. \tag{9}$$

Here, the angle of incidence θ_{i} and the angle of transmission θ_{t} are determined as follows:

$$\cos\theta_{\mathrm{t}} = \frac{n \cos u - 1}{\sqrt{1 - 2n \cos u + n^2}}, \qquad \sin\theta_{\mathrm{i}} = \frac{\sin\theta_{\mathrm{t}}}{n}. \tag{10}$$

The value $D(l)$ describes the convergence of the ray beam. In general, $D(l)$ can be calculated via Fock's formulas containing the first and the second quadratic forms of the surface (5) [17]. However, in the case under consideration, this value can be obtained from simple geometrical considerations. Because the problem is symmetric in φ, it is sufficient to calculate the relation between the segment d_0 (at the point where the ray originates when $l = 0$) and the segment d at the distance l for two closely set rays [see Fig. 1(d)]:

$$\sqrt{D(0)/D(l)} = d_0/d = |1 - l/r(u^*)|^{-1}. \tag{11}$$

As shown in (8) and (11), the ray optics approach gives an infinite field at the focus because $l = r(u^*)$ at this point. In other words, this approach is not applicable near the focus.

To determine the field behavior near the focus, we will utilize the aperture integration technique (a generalization of the Kirchhoff method for vector fields) [16]. Using the ray optics formula (8), we calculate the field distribution over the plane $z = 0$. Because of the ray convergence and the limitedness of the target, the field in the plane $z = 0$ is nonzero only over the limited aperture S_{a}, which is an area enclosed between two circles with radii $\rho_{1,2} = z_{\mathrm{f}} \tan\alpha_{1,2}$, where $\sin\alpha_1 = a/r(u_{\min})$, and $\sin\alpha_2 = \rho_{\max}/r(u_{\max})$. The field at an arbitrary point ρ, φ, $z > 0$ is calculated via the following aperture integral [16]:

$$4\pi\vec{E}_\omega = \frac{i}{k} \iint_{S_{\mathrm{a}}} ([\vec{e}_z, \vec{H}^{\mathrm{a}}_\omega], \nabla') \nabla' g\, d\Sigma' + ik \iint_{S_{\mathrm{a}}} g[\vec{e}_z, \vec{H}^{\mathrm{a}}_\omega] d\Sigma' - \iint_{S_{\mathrm{a}}} [[\vec{E}^{\mathrm{a}}_\omega, \vec{e}_z], \nabla' g] d\Sigma', \tag{12}$$

where the prime symbol indicates that differentiation and integration are performed over the primed coordinates of the point at the aperture, $g = \exp(ik\tilde{R})/\tilde{R}$,

$$\tilde{R} = \sqrt{\rho^2 + \rho'^2 - 2\rho\rho' \cos(\varphi - \varphi') + (z - z')^2}, \tag{13}$$

$\vec{H}^{\mathrm{a}}_\omega$ and $\vec{E}^{\mathrm{a}}_\omega$ are calculated via (6)–(8) with

$$\theta = \theta_{\mathrm{a}} = \pi - \arctan(\rho/z_{\mathrm{f}}), \qquad R = R_{\mathrm{a}} = \sqrt{\rho^2 + z_{\mathrm{f}}^2}. \tag{14}$$

Note that integral (12) can be calculated numerically.

Note that both of these methods only account for a single refracted ray, whereas, strictly speaking, the field is formed by multiple refracted rays [Fig. 1(d)]. However, these additional rays cannot be concentrated by the target, which only concentrates parallel rays whose angle is α [Fig. 1(c)]. The multiple other refracted rays are not parallel and have angles differ from α. Therefore, the field near the focus (which is the main interest) is not affected by these rays in practice.

Figure 2 shows the behavior of the field for a single ray calculated using the two discussed approaches. Note that the permittivity of the real target material (Teflon) is used, and the losses in this material are taken into account. We also have chosen the bunch with a charge 100 pC that can pass through a millimeter-size channel [8]. As we can see, the ray optics approach shows an infinite field at the focus (as formulas (8) and (11) predict), while the aperture integration technique shows a finite field. The two methods are in a good agreement (excluding the narrow vicinity of the peaks center). The larger frequencies correspond to better agreements between curves. For increasing values of ω, the width of the peak decreases (the height of the peak decreases too because the ratio between a and a wavelength $\lambda \sim \omega^{-1}$ increases). Detailed tracing of the curves in Fig. 2 shows that the field at the focus can be approximately 2

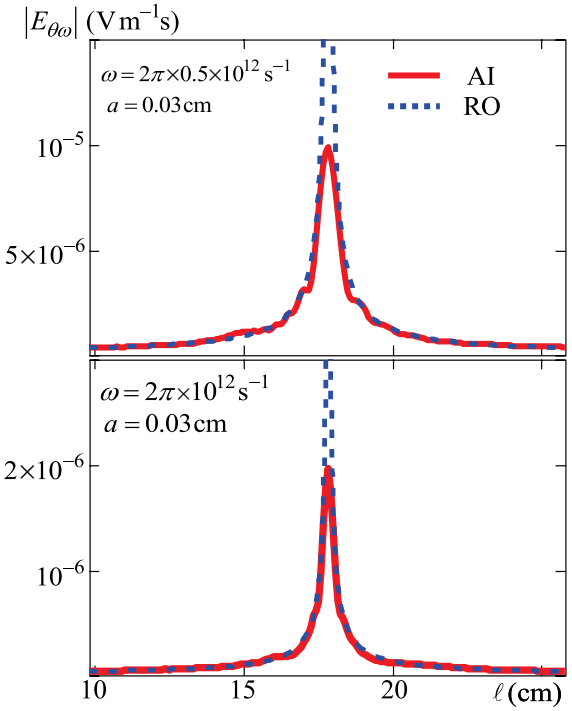

FIG. 2 (color online). Field behavior along the ray determined by the angle $\theta = 170°$ calculated via the ray optics formulas (8) (RO) and the aperture integration approach (12) (AI). Problem parameters: $|q| = 100$ pC, $\varepsilon = 2 + 0.001i$, $\mu = 1$ (Teflon), $\beta = 0.8$, $x_{\max} = 25$ cm, $z_f = 8.3$ cm, $f = 5$ cm. The value $l = 17.8$ cm corresponds to the focus point.

orders of magnitude larger than the field at the surface of the target.

For a more detailed illustration of the concentrating properties of the target, we have calculated a two-dimensional field distribution (Fig. 3). As we can see, the field is especially concentrated in a small area near the focus point $\rho = 0$, $z = z_f$. For the parameters of Fig. 3, the focal spot (which is estimated to be on the order of 10^{-6}) is

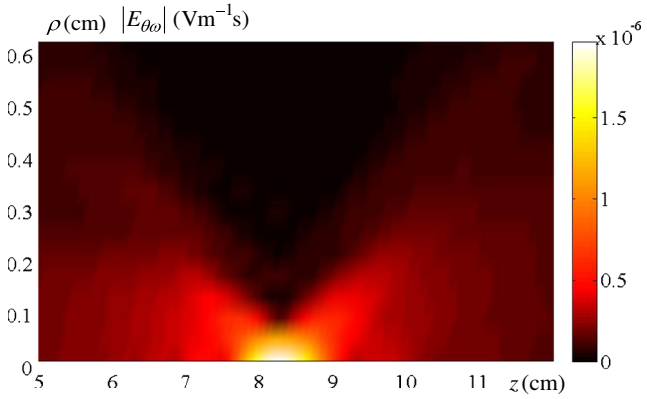

FIG. 3 (color online). Distribution of the absolute value of the field $|E_\theta|$ calculated using the aperture integration approach (12). The frequency $\omega = 2\pi \times 10^{12}$ s^{-1}, $a = 0.03$ cm, and the other problem parameters are the same as in Fig. 2.

approximately 1 cm in the longitudinal direction and 0.1 cm in the orthogonal direction. For the results shown in Fig. 3, we can expect further compaction of the focus spot as the radiation frequency increases.

In Fig. 3, the field exhibits the main maximum at the focus and a lot of weaker maxima. These lateral maxima are explained by the fact that each point of the aperture works as an elementary radiator (in accordance with the aperture method). In the case under consideration where the aperture is excited by a quasiplane wave (8), the elementary radiator consists of crossed magnetic and electric point dipoles. The interference of the fields produced by these dipoles causes the oscillation of the field.

In conclusion, we determined the specific shape of a cylindrically symmetric dielectric target that concentrates the CR produced by a charge into a specific small spatial area. Using the aperture integration technique, we have calculated the field in the space surrounding the target, including the area near the focus (where the ray optics approach fails). We have presented a typical two-dimensional field distribution and have estimated the focal spot. For a decimeter-sized target and a radiated frequency of approximately 1 THz, the size of the focal spot was approximately 1×0.1 cm^2. Increases in the radiation frequency should lead to further decreases in the size of the focal spot and better energy concentration.

This work was supported by the Grant of the President of Russian Federation (No. 273.2013.2) and Grant of St. Petersburg State University (No. 11.0.61.2010).

*galiaminsn@yandex.ru
†tyukhtin@bk.ru

[1] J. V. Jelley, *Čerenkov Radiation and its Applications* (Pergamon, New York, 1958).
[2] V. P. Zrelov, *Vavilov-Cherenkov Radiation in High-Energy Physics* (Israel Program for Scientific Translations, Jerusalem, 1970).
[3] A. P. Potylitsyn, Y. A. Popov, L. G. Sukhikh, G. A. Naumenko, and M. V. Shevelev, J. Phys. Conf. Ser. **236**, 012025 (2010).
[4] A. P. Potylitsyn, S. Y. Gogolev, D. V. Karlovets, G. A. Naumenko, Y. A. Popov, M. V. Shevelev, and L. G. Sukhikh, in *Proceedings of the International Particle Accelerator Conference (IPAC'2010), Kyoto, Japan, 2010* p. 1074, http://accelconf.web.cern.ch/AccelConf/IPAC10/index.htm.
[5] S. Antipov, C. Jing, M. Fedurin, W. Gai, A. Kanareykin, K. Kusche, P. Schoessow, V. Yakimenko, and A. Zholents, Phys. Rev. Lett. **108**, 144801 (2012).
[6] B. Jiang, C. Jing, P. Schoessow, J. Power, and W. Gai, Phys. Rev. ST Accel. Beams **15**, 011301 (2012).
[7] G. P. Gallerano and S. Biedron, in *Proceedings of the Free Electron Laser Conference* p. 216, www.jacow.org.
[8] S. Antipov, M. Babzien, C. Jing, M. Fedurin, W. Gai, A. Kanareykin, K. Kusche, V. Yakimenko, and A. Zholents, Phys. Rev. Lett. **111**, 134802 (2013).

[9] A. A. Ponomarenko, M. I. Ryazanov, M. N. Strikhanov, and A. A. Tishchenko, Nucl. Instrum. Methods Phys. Res., Sect. B **309**, 223 (2013).
[10] A. E. Spinelli, F. Boschi, D. D'Ambrosio, L. Calderan, M. Marengo, A. Fenzi, M. Menegazzi, A. Sbarbati, A. Del Vecchio, and R. Calandrino, Nucl. Instrum. Methods Phys. Res., Sect. A **648**, S310 (2011).
[11] B. M. Bolotovskii, Uspekhi Fizicheskikh Nauk **62**, 201 (1957).
[12] B. M. Bolotovskii, Physics-Uspekhi **4**, 781 (1962).
[13] A. A. Tishchenko, A. P. Potylitsyn, and M. N. Strikhanov, Phys. Rev. E **70**, 066501 (2004).
[14] D. V. Karlovets, JETP **113**, 27 (2011).
[15] E. S. Belonogaya, A. V. Tyukhtin, and S. N. Galyamin, Phys. Rev. E **87**, 043201 (2013).
[16] A. Z. Fradin, *Microwave Antennas* (Pergamon, New York, 1961).
[17] V. A. Fok, *Electromagnetic Diffraction and Propagation Problems* (Pergamon, New York, 1965).